



# The Clusters Hiding in Plain Sight (CHiPS) Survey: CHIPS1911+4455, a Rapidly Cooling Core in a Merging Cluster

Taweewat Somboonpanyakul<sup>1</sup>, Michael McDonald<sup>1</sup>, Matthew Bayliss<sup>2</sup>, Mark Voit<sup>3</sup>, Megan Donahue<sup>3</sup>, Massimo Gaspari<sup>4,5</sup>, Håkon Dahle<sup>6</sup>, Emil Rivera-Thorsen<sup>6</sup>, and Antony Stark<sup>7</sup>

<sup>1</sup> Kavli Institute for Astrophysics and Space Research, Massachusetts Institute of Technology, 77 Massachusetts Avenue, Cambridge, MA 02139, USA

<sup>2</sup> Department of Physics, University of Cincinnati, Cincinnati, OH 45221, USA

<sup>3</sup> Physics & Astronomy Department, Michigan State University, East Lansing, MI 48824-2320, USA

<sup>4</sup> INAF, Osservatorio di Astrofisica e Scienza dello Spazio, via P. Gobetti 93/3, I-40129 Bologna, Italy

<sup>5</sup> Department of Astrophysical Sciences, Princeton University, Princeton, NJ 08544, USA

<sup>6</sup> Institute of Theoretical Astrophysics, University of Oslo, P.O. Box 1029, Blindern, NO-0315 Oslo, Norway

<sup>7</sup> Center for Astrophysics | Harvard & Smithsonian, 60 Garden Street, Cambridge MA 02138, USA

Received 2020 November 6; revised 2020 December 18; accepted 2020 December 20; published 2021 January 19

## Abstract

We present high-resolution optical images from the Hubble Space Telescope, X-ray images from the Chandra X-ray Observatory, and optical spectra from the Nordic Optical Telescope for a newly discovered galaxy cluster, CHIPS1911+4455, at  $z = 0.485 \pm 0.005$ . CHIPS1911+4455 was discovered in the Clusters Hiding in Plain Sight survey, which sought to discover galaxy clusters with extreme central galaxies that were misidentified as isolated X-ray point sources in the ROSAT All-Sky Survey. With new Chandra X-ray observations, we find the core ( $r = 10$  kpc) entropy to be  $17^{+2}_{-9}$  keV cm<sup>2</sup>, suggesting a strong cool core, which is typically found at the centers of relaxed clusters. However, the large-scale morphology of CHIPS1911+4455 is highly asymmetric, pointing to a more dynamically active and turbulent cluster. Furthermore, the Hubble images reveal a massive, filamentary starburst near the brightest cluster galaxy (BCG). We measure the star formation rate for the BCG to be  $140\text{--}190 M_{\odot} \text{ yr}^{-1}$ , which is one of the highest rates measured in a central cluster galaxy to date. One possible scenario for CHIPS1911+4455 is that the cool core was displaced during a major merger and rapidly cooled, with cool, star-forming gas raining back toward the core. This unique system is an excellent case study for high-redshift clusters, where such phenomena are proving to be more common. Further studies of such systems will drastically improve our understanding of the relation between cluster mergers and cooling, and how these fit in the bigger picture of active galactic nuclei feedback.

*Unified Astronomy Thesaurus concepts:* Galaxy clusters (584); Starburst galaxies (1570)

## 1. Introduction

Early X-ray observations of the intracluster medium (ICM) in the center of galaxy clusters revealed cooling times much shorter than the Hubble time, leading to the development of the cooling flow model (e.g., Fabian 1994). In this model, hot gas in dense cores should radiatively cool and fuel  $100\text{--}1000 M_{\odot} \text{ yr}^{-1}$  starbursts in the central brightest cluster galaxy (BCG). However, many studies have shown that BCGs are only forming stars at  $\sim 1\%$  of this rate (e.g., McDonald et al. 2018). A promising mechanism proposed for preventing cooling of the ICM is active galactic nucleus (AGN) heating by jets and bubble-induced weak shocks (see reviews by Fabian 2012; McNamara & Nulsen 2012; Gaspari et al. 2020). Evidence supporting these theories includes the ubiquitous presence of radio galaxies at the center of clusters (Sun 2009) and the similarity between the mechanical energy released by AGN-driven bubbles and the energy needed to quench cooling (e.g., Bîrzan et al. 2008; Rafferty et al. 2008; Hlavacek-Larrondo et al. 2015).

Galaxy clusters with signatures of cooling in their centers are often called “cool-core” (CC) clusters, with their counterparts being referred to as “non-cool-core” (NCC) clusters. Hudson et al. (2010) found that the best way to segregate the two is to consider their central cooling time ( $t_{\text{cool}}$ ). Specifically, CC clusters have  $t_{\text{cool}} < 7.7$  Gyr, while clusters with  $t_{\text{cool}} < 1.0$  Gyr are referred to as “strong CCs.” A number of observational studies have found that CCs are mostly found in relaxed clusters while NCCs reside in dynamically active clusters.

Indeed, all of the strongest CCs known (based on cooling rate) are found in the most relaxed clusters (e.g., Phoenix, McDonald et al. 2012; A1835, McNamara et al. 2006; Zw3146, Edge et al. 1994). This is also consistent with a variety of other studies that found star-forming BCGs in the most relaxed CC clusters (Crawford et al. 1999; Donahue et al. 2010; Molendi et al. 2016; Cerulo et al. 2019). On the other hand, morphologically disturbed clusters (which are likely to be recent mergers) generally have no evidence for ongoing cooling, suggesting that major mergers may have the potential to destroy cool cores (Burns et al. 2008; Poole et al. 2008) through shock-heating (Burns et al. 1997) and mixing (Gómez et al. 2002).

The discovery of CHIPS1911+4455 (Somboonpanyakul et al. 2021) runs counter to these established norms, since it not only harbors a very blue (star-forming) galaxy in the center, but also shows a highly disturbed morphology on both large ( $\sim 200$  kpc) and small ( $\sim 20$  kpc) scales. There are no known nearby clusters that have properties similar to CHIPS1911+4455, though McDonald et al. (2016) report a higher fraction of star-forming BCGs in merging clusters at  $z > 1$ . This implies that CHIPS1911+4455 may provide an avenue for studying a high-redshift phenomenon in a low-redshift cluster. To fully understand this system we have obtained new observations in the core of CHIPS1911+4455, which we will discuss below.

Throughout this Letter, we assume  $H_0 = 70 \text{ km s}^{-1} \text{ Mpc}^{-1}$ ,  $\Omega_m = 0.3$ , and  $\Omega_{\Lambda} = 0.7$ . All errors are  $1\sigma$  unless noted otherwise.

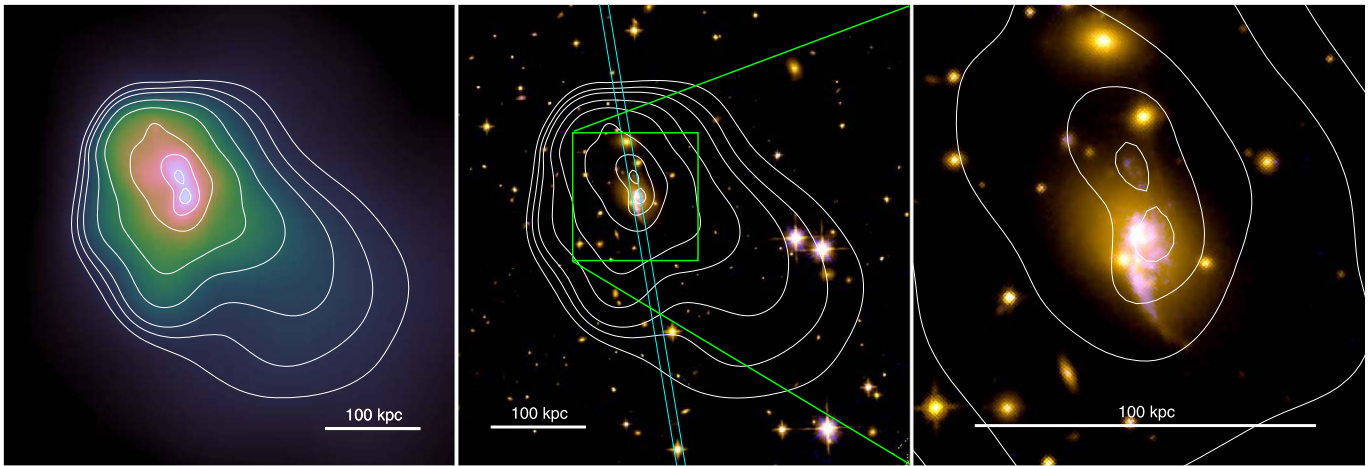


**Figure 1.** Left: Chandra 0.5–7.0 keV image of CHIPS1911+4455, highlighting the asymmetric morphology on both small and large scales. The image is oriented such that north is up and east is to the left. Middle: Hubble images with X-ray contours overlaid. The contour lines were chosen arbitrarily to guide the eye. The cyan box shows the orientation of the long slit (see also Figure 5). Right: the Hubble images of the central galaxy, showing the blue star-forming filaments, extending on scales of  $\sim 30$  kpc. These images show that the cool, star-forming gas is centered on the X-ray peak, with a faint set of filaments extending north to the secondary peak and a brighter filament extending to the south.

## 2. Observations

In this section, we summarize the acquisition and reduction of data obtained from the Chandra X-ray telescope, the Hubble Space Telescope, and the Nordic Optical Telescope (NOT).

### 2.1. X-Ray: Chandra

CHIPS1911+4455 (OBSID: 21544) was observed in 2019 with Chandra ACIS-I for a total of 30.5 ks. The data were analyzed with CIAO v4.11 and CALDB v4.8.5 and recalibrated with VFAINT mode for improved background screening. To look for small-scale structures near the center of the cluster, images were smoothed adaptively, using CSMOOTH<sup>8</sup> to achieve a uniform signal-to-noise ratio over the full image, as shown in the left panel of Figure 1.

The temperature profile was extracted from coarse annuli so that the number of counts per annulus was around 800, which is enough to get well-constrained temperature measurements ( $\Delta kT/kT \sim 20\%$ ). All spectra were fit simultaneously with the APEC model for the cluster emission, a second APEC model for the Milky Way ( $kT = 0.18$  keV), the PHABS model for Galactic absorption, and the BREMSS model to represent a hard background ( $kT = 0.40$  keV) from unresolved point sources, following McDonald et al. (2013). The WSTAT statistic was used.

The gas density profile was created by first computing the 0.7–2.0 keV surface brightness profile. The conversion from the X-ray surface brightness profile to the emission-measure profile ( $EM(r) = \int n_p n_e dl$ ) was calculated as a function of radius based on the best-fit temperature profile and assuming a collisionally ionized plasma APEC model with metallicity  $0.3Z_\odot$ . For more details of the X-ray analysis, see Somboonpanyakul et al. (2018).

### 2.2. Optical: Hubble

CHIPS1911+4455 was observed for two orbits with the Hubble Space Telescope (HST) during Cycle 27. The data

include mediumband F550M data from the Advance Camera for Surveys (ACS) and broadband F110W data from the Wide Field Camera infrared channel (WFC3-IR). The F550M filter contains both the blue continuum and the bright [O II] doublet at the redshift of the cluster, which should both be elevated in star-forming regions. The F110W filter, on the other hand, is sensitive to the red continuum, probing the old stellar populations of the BCG and other cluster members.

### 2.3. Optical Spectra: Nordic Telescope

Two optical spectra of the BCG of CHIPS1911+4455 were obtained with the Alhambra Faint Object Spectrograph and Camera (ALFOSC) at the 2.56 m Nordic Optical Telescope (NOT) on 2019 May 9. One of the spectra was obtained from Grism #4 ( $R = 360$ , 3200–9600 Å) with  $1''.3$  slit for 1500 s exposure. The other spectrum was a stack of two 1100 s spectra from Grism #5 ( $R = 415$ , 5000–10700 Å) with  $1''.3$  slit at  $90^\circ$  from the first spectrum. Wavelength solutions for the two spectra were calibrated with HeNe and ThAr arc lamps, respectively, with an absolute calibration uncertainty of 2 Å. Masks were applied to remove cosmic rays before the 1D spectra were extracted from the 2D spectral images. The 1D spectra were then flat-fielded, and background-subtracted from off-source regions surrounding the 1D extraction region.

## 3. Results

### 3.1. CHIPS1911+4455: A Strong Cool Core

The thermodynamic profiles of CHIPS1911+4455 are shown in Figure 2. The electron density at 10 kpc is  $0.0884 \text{ cm}^{-3}$ , which is among the highest measured to date (Hudson et al. 2010; McDonald et al. 2017), while the temperature profile drops from a maximum of  $\sim 8$  keV at  $\sim 300$  kpc to 4 keV at  $\sim 10$  kpc.

The entropy of the ICM ( $K \equiv kTn_e^{-2/3}$ ) reflects the thermal history of a cluster, which is solely affected by heat gains and losses (Cavagnolo et al. 2009; Panagoulia et al. 2014), while the cooling time ( $t_{\text{cool}} \equiv \frac{3(n_e + n_p)kT}{2n_e n_p \Lambda(T)}$ ) represents the amount of time required for the ICM to radiate all the excess heat, where

<sup>8</sup> <https://cxc.harvard.edu/ciao/ahelp/csmooth.html>

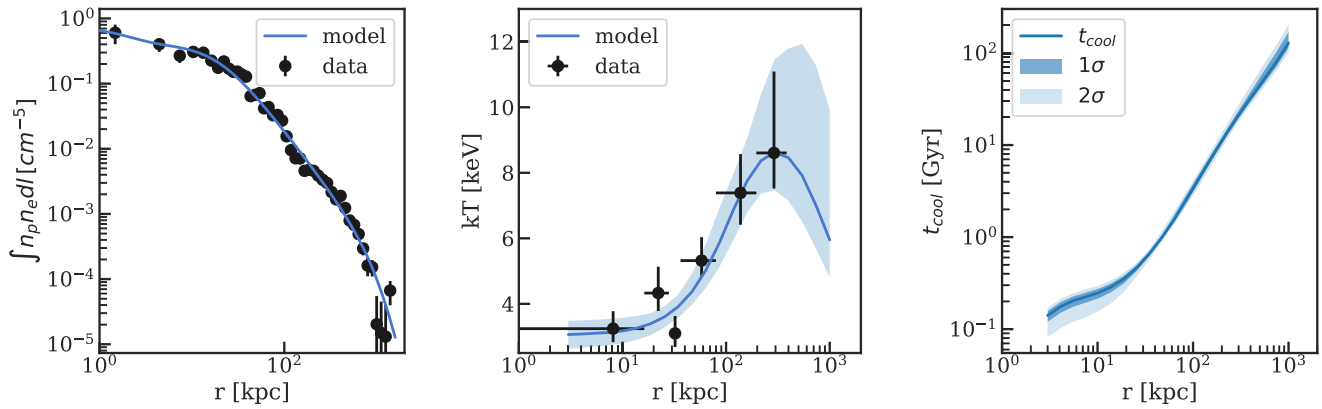


**Figure 2.** Left: the surface brightness profile of CHIPS1911+4455. The black dots are data points, and the blue line is the best-fit model (see Somboonpanyakul et al. 2018 for a further description of this modeling). Middle: the projected 2D temperature profile of the cluster. The black dots are data extracted from modeling of the X-ray spectra. The blue line is the best-fit model following Vikhlinin et al. (2006). Right: the cooling time profile of the cluster. The cyan shaded region corresponds to  $1\sigma$  credible region from the models in the left and middle panels, while the light blue shaded region corresponds to the  $2\sigma$  credible region. This cluster is classified as a strong cool core, based on a large drop in the core temperature and a central cooling time less than 1 Gyr (Hudson et al. 2010).

$\Lambda(T)$  is the cooling function (Sutherland & Dopita 1993). For CHIPS1911+4455, the central ( $r=10$  kpc) cooling time is  $98_{-32}^{+7}$  Myr, which is classified as a strong cool core (Hudson et al. 2010). The deprojected entropy profiles for CHIPS1911+4455, the Phoenix cluster, and hundreds of clusters from the ACCEPT survey (Cavagnolo et al. 2009) are shown in Figure 3. Both CHIPS1911+4455 and the Phoenix cluster have entropy profiles that are among the lowest known. The core ( $r=10$  kpc) entropy for CHIPS1911+4455 is  $17_{-9}^{+2}$  keV cm<sup>2</sup>, which is in the 5th percentile of all clusters in the ACCEPT survey.

### 3.2. CHIPS1911+4455: A Major Merger

There are various ways to quantify the dynamical state of a cluster, with some of the best combining X-ray data with information on the galaxy velocities. Lacking the latter, we restrict ourselves to X-ray-only indicators. The two particular quantities we consider are the “peakiness” of the surface brightness profile and the distance between the center of symmetry on small and large scales (“symmetry”), following Mantz et al. (2015). The peakiness measure is a proxy for the presence of a cool core, which is typically found in relaxed clusters. A cluster with high symmetry appears similar on small and large scales, suggesting that it is dynamically relaxed. Given that both of these proxies probe the dynamical state of the cluster, albeit in different ways, it is unsurprising that they are correlated (Mantz et al. 2015). The green points in Figure 4 show the population of relaxed clusters in this morphology plane. For CHIPS1911+4455, the peakiness is measured to be  $-0.501$ , which is in the 96th percentile of all clusters, while the symmetry is estimated to be  $0.425$ , which is in the 7th percentile. The fact that CHIPS1911+4455 is simultaneously one of the strongest cool cores *and* least symmetric clusters known is highly unusual.

### 3.3. CHIPS1911+4455: A Starburst BCG

In Figure 1, we compare optical and X-ray images of CHIPS1911+4455. The Hubble images show that the red emission from old stellar populations is relatively smooth and symmetric, while the blue emission from the young stellar

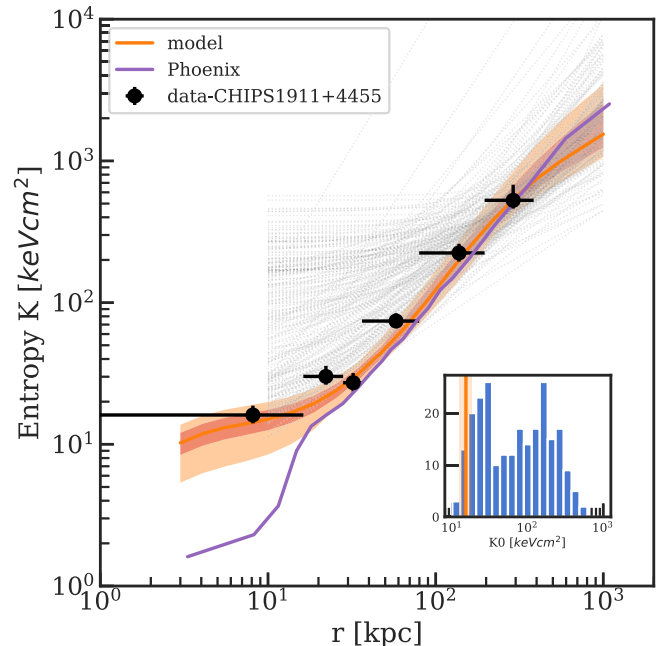


**Figure 3.** Entropy profile for CHIPS1911+4455 (orange), compared to 239 clusters from the ACCEPT survey (gray; Cavagnolo et al. 2009) and the Phoenix cluster (purple; McDonald et al. 2019). The shaded region corresponds to  $1\sigma$  and  $2\sigma$  credible regions (see Figure 2). The black dots are data points, estimated from the projected 2D temperature data and the 3D density model. The inset shows the histogram of the core entropy ( $r < 10$  kpc) of all the ACCEPT clusters and CHIPS1911+4455 (orange). CHIPS1911+4455’s core entropy is in the lowest 10% of all ACCEPT clusters.

populations and cool gas is clumpy, asymmetric, and extended on  $>30$  kpc scales. In particular, the red emission shows no elongation toward the galaxies to the north, suggesting that there has not been a recent interaction between these galaxies. Given this, and the fact that the central entropy is among the  $\sim 2$ – $3$  lowest ever measured, we propose that the young stars are forming directly from the cooling ICM. The filamentary complex structures in the blue emission are similar to the emission nebula in the Phoenix cluster (McDonald et al. 2019) and other nearby cool-core clusters (e.g., McDonald et al. 2011; Tremblay et al. 2015; Olivares et al. 2019).

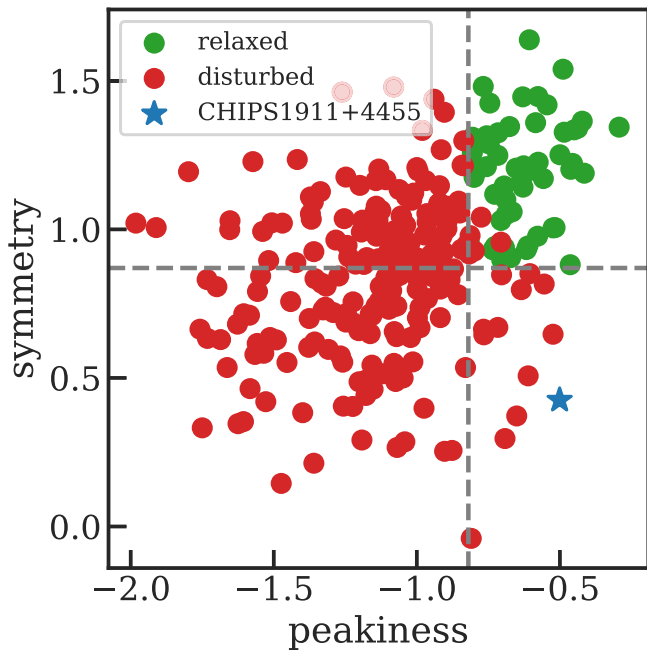


**Figure 4.** Distribution of X-ray symmetry and peakiness for clusters presented in Mantz et al. (2015). Dashed lines show the cuts used to define the relaxed sample, which were chosen to broadly agree with “by-eye” assessments of relaxedness. Clusters satisfying this criterion are shown in green, while red points show the nonrelaxed clusters. The blue star represents the location of CHIPS1911+4455, which is the peakiest cluster with large-scale asymmetry.

From the optical spectrum in Figure 5, we identify several bright emission lines, including  $H\beta$  and  $[O II]$ . The relative lack of bright  $[O III]$  compared to  $[O II]$  indicates that the central galaxy in CHIPS1911+4455 is a massive starburst and not a bright AGN. We use these emission lines to estimate the redshift of the central galaxy, finding  $z = 0.485 \pm 0.005$ . From the two slit orientations, we measure  $[O II]$  equivalent widths of  $40.9 \pm 1.0 \text{ \AA}$  and  $43.8 \pm 1.0 \text{ \AA}$ , which are consistent with one another. To convert to flux, we model the spectral energy distribution (SED) of the galaxy, based on data from Pan-STARRS ( $g$ ,  $i$ ,  $r$ ,  $z$ , and  $y$ ; Tonry et al. 2012) and WISE ( $w1$  and  $w2$ ; Wright et al. 2010), with a linear combination of “young” and “old” stellar populations, along with dust reddening (Calzetti et al. 2000). The best-fit SED model is shown in Figure 5. We estimate a dereddened continuum flux at the location of  $[O II]$  of  $3.5 \pm 0.5 \times 10^{-16} \text{ erg s}^{-1} \text{ cm}^{-2} \text{ \AA}^{-1}$ , which we combine with the EW to estimate the star formation rate (SFR) of the central galaxy, arriving at  $189_{-22}^{+25} M_{\odot} \text{ yr}^{-1}$  (Kennicutt 1998).

Another way to measure SFR is to use the  $24 \mu\text{m}$  emission since mid-IR fluxes are unaffected by dust extinction, unlike UV and optical tracers. Instead, mid-IR emission comes from the reprocessed light by dust, produced from recently formed stars. Based on the WISE4 flux ( $\sim 4 \times 10^{-18} \text{ erg s}^{-1} \text{ cm}^{-2} \text{ \AA}^{-1}$ ), we estimate the SFR for the central galaxy to be  $143_{-26}^{+31} M_{\odot} \text{ yr}^{-1}$ , based on Cluver et al. (2017).

Considering both the  $[O II]$  emission line luminosity and the mid-IR continuum, we obtain consistent SFRs of  $\sim 140\text{--}190 M_{\odot} \text{ yr}^{-1}$ , making the BCG in CHIPS1911+4455 one of the most star-forming BCGs in the  $z < 1$  universe (see, e.g., McDonald et al. 2018).

#### 4. Discussion

It is clear, based on Sections 3.1–3.3, that CHIPS1911+4455 is a unique system in the nearby universe ( $z < 0.5$ ) with an extremely high central SFR, a strong cool core, and large-scale morphology consistent with a recent merger. It is common knowledge that, at low redshift, the most star-forming BCGs tend to be located in the most relaxed, cool-core clusters (Cavagnolo et al. 2008; Donahue et al. 2010). Whereas, the SFR in high-redshift BCGs tend to be higher in dynamically active, non-cool-core clusters (McDonald et al. 2016; Bonaventura et al. 2017). CHIPS1911+4455 may represent a low-redshift analog of these high-redshift systems, allowing us to study physical processes that may have been much more common at early times. Below, we speculate on possible explanations for the observed starburst.

In the precipitation scenario (Voit et al. 2015) for AGN feeding and feedback, cool clouds condense and can form stars or fuel AGN feedback when the cooling time ( $t_{\text{cool}}$ ) is significantly shorter than the timescale for the cloud to fall to the center of the cluster potential ( $t_{\text{ff}}$ ). The latter timescale is a proxy for the mixing time of the cooling gas. The threshold for thermal instability is usually taken to be  $t_{\text{cool}}/t_{\text{ff}} < 10$  (e.g., Voit et al. 2015; Gaspari et al. 2020), but this depends on the medium’s susceptibility to condensation, the slope of the entropy profile, the amount of turbulence, and the amplitude of entropy perturbation (Voit et al. 2017; Voit 2018). If a dense, low-entropy core is perturbed from the center of the gravitational potential, the timescale for mixing is increased while the cooling time remains constant, leading to an enhancement in thermal instabilities. Further, the separation of the low-entropy gas from the direct influence of the central AGN could prevent  $t_{\text{cool}}$  from increasing. This displacement of low-entropy gas from the central massive galaxy would happen naturally during a merger (i.e., in CHIPS1911+4455). The X-ray data in Figure 1 support this scenario, depicting a disturbed cool core elongated in the north–south direction. While the bulk of the cool, star-forming gas extends along a southern-pointing filament, there is a fainter blue filament that connects the central BCG to the more northern X-ray peak. This suggests that the northern X-ray peak might contain low-entropy gas that is dislodged from the location of the BCG. The existence of this system—a dynamically active but rapidly cooling core—provides evidence that mergers may stimulate star formation and enhance cooling. This process would be especially relevant in the distant universe when mergers were more common compared to the present time (Fakhouri et al. 2010).

Closely related to this, in the chaotic cold accretion scenario (CCA; e.g., Gaspari et al. 2019) turbulence is a key ingredient to drive direct nonlinear thermal instability and extended condensation. During CCA the global driver can be tied not only to AGN feedback, but to mergers too, which can stimulate a significant amount of turbulence (e.g., Lau et al. 2017) and density fluctuations at large injection scales, enabling enhanced condensation.

In summary, there are multiple ways that a recent cluster–cluster merger could enhance cooling: by increasing the fallback time of a low-entropy cloud (lowering  $t_{\text{cool}}/t_{\text{ff}}$ ), by physically separating the cool gas and the heat source (AGN), and by increasing the local turbulence, leading to larger density fluctuations. The inclusion of dynamically active clusters in the

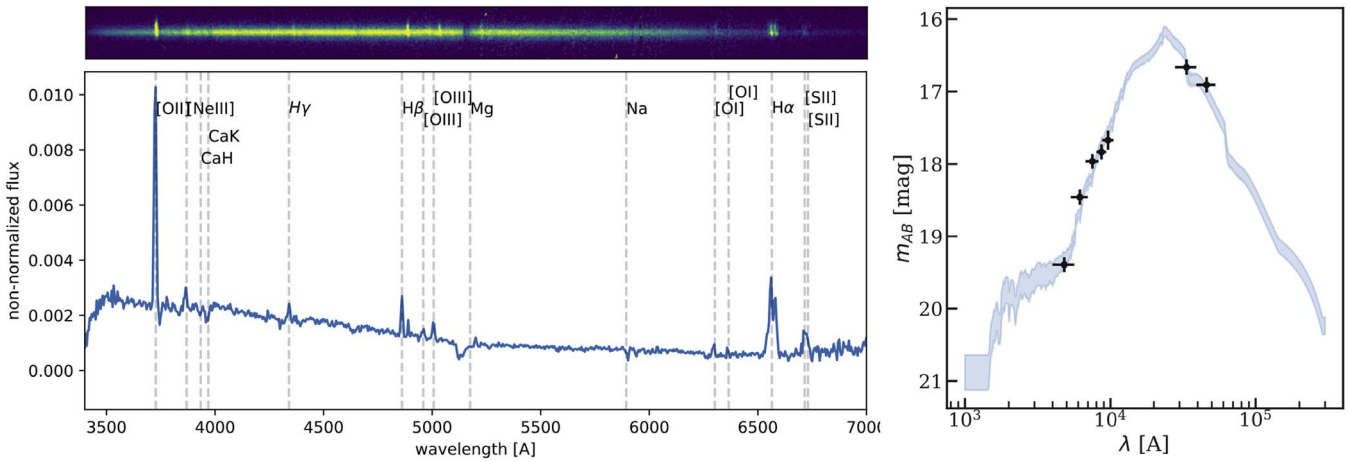


**Figure 5.** Top left: the 2D spectral image of the BCG of CHIPS1911+4455 from the Nordic Optical Telescope showing that the line-emitting gas is extended along the slit (vertical) direction. This confirms that the [O II] emission is not coming (exclusively) from a central AGN, and that the extended emission in Figure 1 is indicating the presence of cool gas, rather than purely blue continuum from young stars. Bottom left: the 1D spectrum in the rest frame from the 2D spectral image above. Gray dashed lines show the location of well-known emission lines. The spectrum clearly shows the strong [O II] doublet at 3727 Å and the H $\alpha$  emission line at 6562.8 Å. Right: the fitted spectral energy distribution (SED) model with broadband optical data ( $g$ ,  $r$ ,  $i$ ,  $z$ , and  $y$ ) from Pan-STARRS and mid-IR from WISE.

suite of high-resolution, zoom-in simulations that study the detailed interplay between radio-loud AGN and the cooling, multiphase ICM (e.g., Gaspari et al. 2019), is a necessary next step toward understanding the relative importance of these phenomena.

## 5. Conclusion

In this work, we present new data from Hubble, Chandra, and the Nordic Optical Telescope. Our findings are summarized as follows:

1. We measure the ICM density in the core ( $r < 10$  kpc) of CHIPS1911+4455 to be  $0.09 \text{ cm}^{-3}$ , which is typical for a cool-core cluster. The core entropy is  $17^{+2}_{-9} \text{ keV cm}^2$ , which is within the lowest 10% for cluster cores from the ACCEPT samples (Cavagnolo et al. 2009). The low-entropy core is a clear signature of strong cooling in the center of the cluster.
2. The X-ray morphology of CHIPS1911+4455 is highly peaked in the center (96th percentile for “peakiness”) and very asymmetric (7th percentile for “symmetry”) compared to a large sample of X-ray-selected clusters. This contradiction in its morphology between a relaxed (peaky) cluster and a dynamically active (asymmetric) cluster is highly unusual, and is rarely observed.
3. Based on the [O II] emission line luminosity, we measure an SFR in the BCG of  $189^{+25}_{-22} M_{\odot} \text{ yr}^{-1}$ . This is consistent with an estimate based on the mid-IR continuum of  $143^{+31}_{-26} M_{\odot} \text{ yr}^{-1}$ . This BCG is among the five most star-forming BCGs in the low- $z$  universe. Data from Hubble confirm that this emission is extended in complex blue filaments near the BCG, with no evidence for an ongoing merger.
4. Based on the highly asymmetric X-ray morphology on small ( $\sim 20$  kpc) scales, coupled with the exceptionally low core entropy, we propose that rapid cooling in this system may have been triggered by a dynamical interaction between two similar-mass clusters. In this scenario, some of the low-entropy gas from the more massive cluster is



dislodged from the central AGN-hosting galaxy. For the low-entropy gas separated from the central galaxy, cooling is more favorable due to the longer mixing times, enhanced large-scale turbulence and CCA rain, and lack of a direct heat source (AGN). This system may provide a link to high-redshift clusters, where previous studies have found an abundance of star-forming BCGs in dynamically active clusters.

CHIPS1911+4455 is the first low-redshift ( $z < 1$ ) galaxy cluster with this distinctive characteristic (hosting a high star-forming BCG and a strong cool-core but having a disturbed morphology). The cluster was discovered by the Clusters Hiding in Plain Sight (CHiPS) survey because of its exceptionally bright cool core that appears to be pointlike in previous X-ray cluster catalogs (Somboonpanyakul et al. 2018). CHIPS1911+4455 represents a unique opportunity to understand the relationship between a merging galaxy cluster and star formation in its BCG, which, in turn, unravels an alternative method to form cooling flows and massive starbursts apart from a simple accretion model. This mechanism will become much more important at high redshift ( $z > 1$ ) when the cluster merger rate is significantly higher (Fakhouri et al. 2010; McDonald et al. 2016).

T.S. and M.M. acknowledge support from the Kavli Research Investment Fund at MIT, Chandra Award Number GO9-20116X, and by Hubble Award Number HST-GO-16038. M.G. acknowledges partial support by NASA Chandra GO8-19104X/GO9-20114X and HST GO-15890.020-A. H.D., A.H. D. and E.R.T. acknowledge support from the Research Council of Norway.

## ORCID iDs

Taweewat Somboonpanyakul <https://orcid.org/0000-0003-3521-3631>  
 Michael McDonald <https://orcid.org/0000-0001-5226-8349>  
 Matthew Bayliss <https://orcid.org/0000-0003-1074-4807>  
 Mark Voit <https://orcid.org/0000-0002-3514-0383>  
 Megan Donahue <https://orcid.org/0000-0002-2808-0853>

Massimo Gaspari  <https://orcid.org/0000-0003-2754-9258>  
 Håkon Dahle  <https://orcid.org/0000-0003-2200-5606>  
 Antony Stark  <https://orcid.org/0000-0002-2718-9996>

## References

- Birzan, L., McNamara, B. R., Nulsen, P. E. J., et al. 2008, *ApJ*, **686**, 859  
 Bonaventura, N. R., Webb, T. M. A., Muzzin, A., et al. 2017, *MNRAS*, **469**, 1259  
 Burns, J. O., Hallman, E. J., Gantner, B., et al. 2008, *ApJ*, **675**, 1125  
 Burns, J. O., Loken, C., Gomez, P., et al. 1997, in ASP Conf. Ser. 115, Galactic Cluster Cooling Flows, ed. N. Soker (San Francisco, CA: ASP), 21  
 Calzetti, D., Armus, L., Bohlin, R. C., et al. 2000, *ApJ*, **533**, 682  
 Cavagnolo, K. W., Donahue, M., Voit, G. M., et al. 2008, *ApJL*, **683**, L107  
 Cavagnolo, K. W., Donahue, M., Voit, G. M., et al. 2009, *ApJS*, **182**, 12  
 Cerulo, P., Orellana, G. A., & Covone, G. 2019, *MNRAS*, **487**, 3759  
 Cluver, M. E., Jarrett, T. H., Dale, D. A., et al. 2017, *ApJ*, **850**, 68  
 Crawford, C. S., Allen, S. W., Ebeling, H., et al. 1999, *MNRAS*, **306**, 857  
 Donahue, M., Bruch, S., Wang, E., et al. 2010, *ApJ*, **715**, 881  
 Edge, A. C., Fabian, A. C., Allen, S. W., et al. 1994, *MNRAS*, **270**, L1  
 Fabian, A. C. 1994, *ARA&A*, **32**, 277  
 Fabian, A. C. 2012, *ARA&A*, **50**, 455  
 Fakhouri, O., Ma, C.-P., & Boylan-Kolchin, M. 2010, *MNRAS*, **406**, 2267  
 Gaspari, M., Eckert, D., Etori, S., et al. 2019, *ApJ*, **884**, 169  
 Gaspari, M., Tombesi, F., & Cappi, M. 2020, *NatAs*, **4**, 10  
 Gómez, P. L., Loken, C., Roettiger, K., et al. 2002, *ApJ*, **569**, 122  
 Hlavacek-Larrondo, J., McDonald, M., Benson, B. A., et al. 2015, *ApJ*, **805**, 35  
 Hudson, D. S., Mittal, R., Reiprich, T. H., et al. 2010, *A&A*, **513**, A37  
 Kennicutt, R. C. 1998, *ARA&A*, **36**, 189  
 Lau, E. T., Gaspari, M., Nagai, D., et al. 2017, *ApJ*, **849**, 54  
 Mantz, A. B., Allen, S. W., Morris, R. G., et al. 2015, *MNRAS*, **449**, 199  
 McDonald, M., Allen, S., Bayliss, M., et al. 2017, *ApJ*, **843**, 28  
 McDonald, M., Bayliss, M., Benson, B. A., et al. 2012, *Natur*, **488**, 349  
 McDonald, M., Benson, B. A., Vikhlinin, A., et al. 2013, *ApJ*, **774**, 23  
 McDonald, M., Gaspari, M., McNamara, B. R., et al. 2018, *ApJ*, **858**, 45  
 McDonald, M., McNamara, B. R., Voit, G. M., et al. 2019, *ApJ*, **885**, 63  
 McDonald, M., Stalder, B., Bayliss, M., et al. 2016, *ApJ*, **817**, 86  
 McDonald, M., Veilleux, S., & Mushotzky, R. 2011, *ApJ*, **731**, 33  
 McNamara, B. R., & Nulsen, P. E. J. 2012, *NJPh*, **14**, 055023  
 McNamara, B. R., Rafferty, D. A., & Birzan, L. 2006, *ApJ*, **648**, 164  
 Molendi, S., Tozzi, P., Gaspari, M., et al. 2016, *A&A*, **595**, A123  
 Olivares, V., Salome, P., Combes, F., et al. 2019, *A&A*, **631**, A22  
 Panagoulia, E. K., Fabian, A. C., & Sanders, J. S. 2014, *MNRAS*, **438**, 2341  
 Poole, G. B., Babul, A., McCarthy, I. G., et al. 2008, *MNRAS*, **391**, 1163  
 Rafferty, D. A., McNamara, B. R., & Nulsen, P. E. J. 2008, *ApJ*, **687**, 899  
 Somboonpanyakul, T., McDonald, M., Gaspari, M., Stalder, B., & Stark, A. A. 2021, arXiv:2101.01730  
 Somboonpanyakul, T., McDonald, M., Lin, H. W., et al. 2018, *ApJ*, **863**, 122  
 Sun, M. 2009, *ApJ*, **704**, 1586  
 Sutherland, R. S., & Dopita, M. A. 1993, *ApJS*, **88**, 253  
 Tonry, J. L., Stubbs, C. W., Lykke, K. R., et al. 2012, *ApJ*, **750**, 99  
 Tremblay, G. R., O’Dea, C. P., Baum, S. A., et al. 2015, *MNRAS*, **451**, 3768  
 Vikhlinin, A., Kravtsov, A., Forman, W., et al. 2006, *ApJ*, **640**, 691  
 Voit, G. M. 2018, *ApJ*, **868**, 102  
 Voit, G. M., Donahue, M., Bryan, G. L., et al. 2015, *Natur*, **519**, 203  
 Voit, G. M., Meece, G., Li, Y., et al. 2017, *ApJ*, **845**, 80  
 Wright, E. L., Eisenhardt, P. R. M., Mainzer, A. K., et al. 2010, *AJ*, **140**, 1868